Stem Cell Reports
Report
ISSCR
OPEN ACCESS

Activation of Intrinsic Growth State Enhances Host Axonal Regeneration into Neural Progenitor Cell Grafts

Hiromi Kumamaru,[1] Paul Lu,[1,2] Ephron S. Rosenzweig,[1] and Mark H. Tuszynski[1,2,*]
[1]Department of Neurosciences, University of California – San Diego, 0626, La Jolla, CA 92093, USA
[2]Veterans Administration San Diego Healthcare System, San Diego, CA 92161, USA
*Correspondence: mtuszynski@ucsd.edu
https://doi.org/10.1016/j.stemcr.2018.08.009

SUMMARY

Axonal regeneration after spinal cord injury (SCI) can be enhanced by activation of the intrinsic neuronal growth state and, separately, by placement of growth-enabling neural progenitor cell (NPC) grafts into lesion sites. Indeed, NPC grafts support regeneration of all host axonal projections innervating the normal spinal cord. However, some host axons regenerate only short distances into grafts. We examined whether activation of the growth state of the host injured neuron would elicit greater regeneration into NPC grafts. Rats received NPC grafts into SCI lesions in combination with peripheral "conditioning" lesions. Six weeks later, conditioned host sensory axons exhibited a significant, 9.6-fold increase in regeneration into the lesion/graft site compared with unconditioned axons. Regeneration was further enhanced 1.6-fold by enriching NPC grafts with phenotypically appropriate sensory neuronal targets. Thus, activation of the intrinsic host neuronal growth state and manipulation of the graft environment enhance axonal regeneration after SCI.

INTRODUCTION

Several mechanisms contribute to axon regeneration failure in the adult CNS, including: (1) the absence of permissive substrates for axonal growth in the lesion cavity (Bunge, 2001; Hur et al., 2012; O'Shea et al., 2017), (2) the adult neuron's failure to fully upregulate its intrinsic growth state (He and Jin, 2016; Mar et al., 2014; Tedeschi and Bradke, 2017), and (3) the presence of inhibitors to axon growth in both adult myelin (Filbin, 2003; Lee et al., 2010; Silver et al., 2014) and the surrounding extracellular matrix (Fawcett, 2006; Laabs et al., 2005). Recently we found that grafts of neural progenitor cells (NPCs) to sites of spinal cord injury (SCI) result in regeneration of lesioned host axons into the lesion/graft site (Kadoya et al., 2016; Lu et al., 2014), and extension of graft-derived axons out from the lesion and into the host spinal cord (Lu et al., 2012; Rosenzweig et al., 2018). Both host axons regenerating into grafts, and grafts axons extending into the host, form synapses, and these are electrophysiologically active (Lu et al., 2012). Graft-initiated retrograde trans-synaptic rabies tracing demonstrates that all host systems that normally project to the intact spinal cord also innervate NPC grafts after SCI (Adler et al., 2017). Indeed, functional improvement is observed after grafts of NPCs to either cervical or thoracic injury sites (Kadoya et al., 2016; Lu et al., 2012, 2017; Rosenzweig et al., 2018).

While a diversity of host axonal systems regenerate into NPC grafts placed into sites of SCI, the penetration of some of these host systems is limited to the more superficial regions of grafts, and host axonal regeneration into deeper graft regions is limited; this is particularly true of sensory axons regenerating into NPC grafts (Dulin et al., 2018). Deeper and more extensive regeneration of host axons into NPC grafts could increase the formation of new relay circuits across sites of SCI, leading to improved functional outcomes. A body of previous work has demonstrated that peripheral nerve conditioning lesions significantly enhance regeneration of the central branch of sensory axons after SCI by activating the intrinsic growth state of the injured neuron (Alto et al., 2009; Neumann and Woolf, 1999; Woolf, 2001); interestingly, this enhancement of central sensory axon regeneration is only observed following peripheral, but not central, nerve crush or transection (Seijffers et al., 2007; Woolf, 2001).

In the present study we explored the hypothesis that sensory conditioning lesions activate the intrinsic host neuronal growth state and enhance host axonal regeneration into NPC grafts. Indeed, we find a 9.6-fold increase in sensory axon regeneration into the NPC graft after conditioning lesions. Moreover, enrichment of the graft with target neurons of regenerating sensory axons further enhances regeneration. Collectively, these findings demonstrate that regeneration of injured adult axons into spinal cord lesion sites can be markedly enhanced by modifying both intrinsic neuronal growth state and the graft environment.

RESULTS

We examined regeneration of host sensory axons in neural stem and progenitor cell grafts in two species: rhesus monkeys and Fischer 344 rats. The experimental timeline is shown in Figure S1. Five rhesus monkeys were used to assess the extent to which sensory axons regenerate into

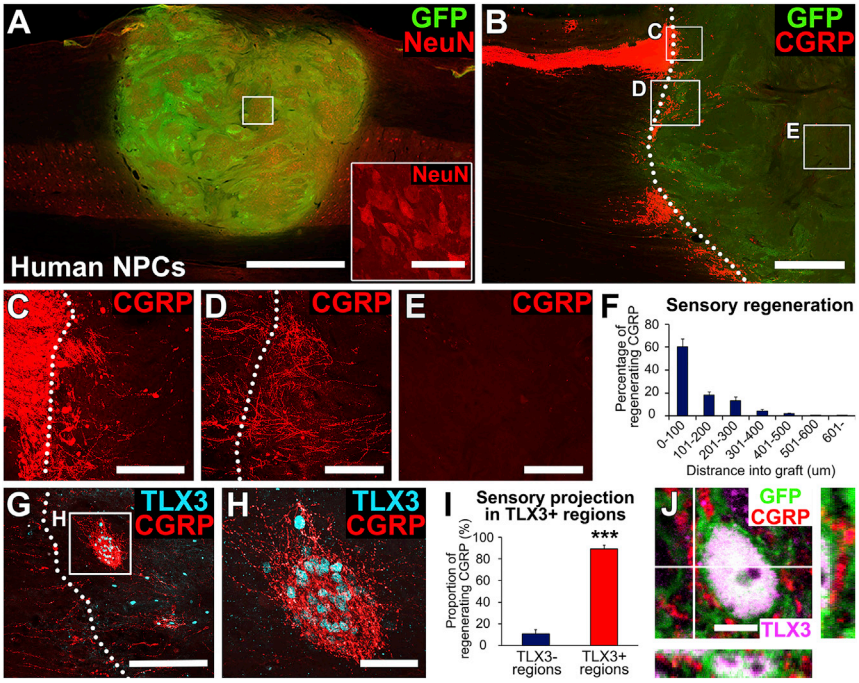

Figure 1. Primate Sensory Axons Regenerate into Specific Target Domains in Human Neural Progenitor Cell Grafts

(A) GFP-expressing human spinal cord multipotent neural progenitor cell (NPC) graft in a C7 hemisection lesion in the rhesus monkey, 3 months after grafting. Horizontal section immunolabeled for GFP (green) and the mature neuronal marker, NeuN (red). Graft survives and fills the lesion site. Left, rostral; right, caudal. Scale bar, 2 mm. Inset shows NeuN expression in the boxed region; scale bar, 50 μm.

(B–E) Primate sensory axons (labeled for CGRP) regenerate into human NPC grafts expressing GFP, but over relatively short distances. (B) Lower-magnification view of sensory axons in the dorsal root entry zone. Left, rostral; right, caudal. Dotted line indicates graft-host border. Scale bar, 1 mm. Boxed areas are shown in (C) to (E). (C) Sensory axons cross host/graft interface and enter graft. (D) Another zone of host sensory axon entry into graft. (E) Core of graft is devoid of regenerating host sensory axons. Scale bars in (C) to (E), 200 μm.

(F) Quantification of CGRP axon regeneration into grafts demonstrates little regeneration beyond 500 μm (n = 5). Data are presented as mean ± SEM.

(G–I) Neurons in regions of sensory axon regeneration express the dorsal sensory interneuronal marker TLX3 (cyan). These cells are clustered. Dotted line indicates graft-host border. Boxed area in (G) is shown at higher magnification in (H). Scale bars, 200 μm (G) and 50 μm (H). (I) Quantification demonstrates that most regenerating host sensory axons penetrate regions of TLX3-expressing cell domains in grafts (n = 5). Data are presented as mean ± SEM. ***p < 0.001. Student's t test.

(J) Immunolabeling for GFP (green), CGRP (red), and TLX3 (purple) reveals that regenerating sensory axons form close appositions with $TLX3^+$ neurons, suggesting synaptic connectivity. Scale bar, 5 μm.

human NPC grafts placed into sites of SCI. As described below, findings demonstrated that adult sensory axons regenerate into human NPC grafts after SCI, but the extent of sensory regeneration is limited to the superficial margins of the graft. We then turned to a rodent model in an effort to enhance the extent of sensory regeneration in NPC grafts after SCI, testing the hypothesis that activation of the intrinsic neuronal growth state induced by peripheral nerve conditioning lesions increases the amount and distance of sensory axon regeneration into grafts.

Primate Sensory Axons Sparsely Regenerate into Phenotypically Appropriate Target Domains in Human NPC Grafts

We previously reported that primary dorsal root ganglia (DRG) sensory axons regenerate into appropriate sensory neuronal target domains within rat multipotent NPC grafts placed into SCI lesions in rats (Dulin et al., 2018). To examine whether this guidance persists in a more clinically relevant species, we grafted human embryonic spinal cord-derived NPCs (see Experimental Procedures) expressing GFP into C7 right hemisection lesion cavities in five rhesus monkeys; grafts were placed 2 weeks after injury. Responses of motor systems to these grafts have recently been published (Rosenzweig et al., 2018). Three months later, grafts filled the lesion cavity and differentiated into NeuN-expressing neurons (Figure 1A). Host calcitonin gene-related peptide $(CGRP)^+$ sensory axons originating from the DRG regenerated into these human NPC grafts (Figures 1B–1F). Notably, these primary sensory axons regenerated into clusters of graft neurons that expressed the specific spinal cord second order sensory neuron transcription factor, TLX3 (Figures 1G and 1H): 89% of regenerating CGRP axons were present in TLX3-expressing graft domains (n = 5, p < 0.001, Student's t test; Figure 1I), and CGRP axon density in TLX3-expressing domains was 5.9-fold higher than in non-TLX3-expressing domains. Host regenerating sensory axons formed close appositions with TLX3-expressing graft neurons (Figure 1J), suggesting synaptic connectivity. However, the extent of sensory axonal

regeneration was modest overall, exhibiting growth only into the first 500 μm of the host/graft interface (Figure 1F); axons did not regenerate into graft cores (Figure 1E). Thus, primate DRG sensory axons regenerate into phenotypically appropriate targets within human NPC grafts after SCI, but this regeneration is modest in extent.

Activation of Host Intrinsic Neuronal Growth State Robustly Enhances Axonal Regeneration into Grafts

Results in the primate model led to an effort to increase the extent of sensory axon regeneration into NPC grafts after SCI. For these experiments, we returned to higher-throughput rat models and tested the hypothesis that increasing the intrinsic growth state of the injured host DRG neuron by conditioning lesions would increase axon regeneration into grafts (Neumann and Woolf, 1999; Woolf, 2001). Ten rats underwent C5 bilateral dorsal spinal cord lesions, and these animals received grafts of embryonic day 14 (E14) spinal cord-derived multipotent NPCs into the lesion site. Half of these animals (n = 5) also received peripheral nerve conditioning lesions the same day (Blesch et al., 2012); conditioning lesions were created by transecting the left musculocutaneous, median, ulnar, and radial nerves, ensuring that most axons projecting into the C5 vertebral segment (C6 and C7 spinal cord segments) were conditioned. Following conditioning lesions, we observed robust enhancement of sensory axon regeneration into grafts: the overall amount of sensory axon regeneration increased 9.6-fold (n = 5 for each group, $p < 0.001$, Student's t test; Figure 2). In the absence of conditioning lesions, sensory axons only regenerated into superficial regions of grafts (Figures 2A–2D), as observed in primates. Moreover, conditioning lesions resulted in host sensory axonal growth through the entirety of the graft (Figures 2E–2H). Once again, axons grew specifically into TLX3-expressing sensory neuronal clusters; 81% of regenerating CGRP axons were present in TLX3-expressing regions of cell clusters (n = 5, $p < 0.001$; Figures 2I, 2J, and 2M). Sensory axons formed bouton-like structures in close apposition to graft TLX3-expressing neurons (Figure 2K); the presence of functional host-graft synapses in TLX3-expressing graft regions was demonstrated in a previous publication by activation of Fos in these neurons following dermal stimulation (Dulin et al., 2018).

We confirmed that conditioning lesions upregulated classic regeneration-associated gene expression (Chong et al., 1992; Mar et al., 2014) in C7 DRGs: indeed, conditioning resulted in a significant, 2-fold increase in expression of GAP-43 (n = 3 replicates, $p < 0.05$; Figures 3A–3C); a significant, 5-fold increase in expression of STAT3 ($p < 0.01$; Figures 3D–3F); and a significant, 29-fold increase in expression of c-Jun ($p < 0.01$; Figures 3G–3I). Thus, activation of the intrinsic growth state of the host neuron significantly and robustly increases axonal regeneration into NPC grafts placed into sites of SCI.

Host Axonal Regeneration Is Further Enhanced by Graft Enrichment with Appropriate Target Domains

Previously we reported that grafts can be enriched in appropriate neuronal target domains for regenerating host sensory axons (Dulin et al., 2018). We next sought to determine whether the combination of conditioning lesions plus enrichment of neural progenitor grafts with appropriate neuronal targets would further enhance host axonal regeneration. To enrich grafts with appropriate, TLX3-expressing neurons, we dissected E14 spinal cords into dorsal or ventral halves: dorsal halves contain TLX3-expressing progenitors of primary sensory axons, whereas ventral halves are depleted in TLX3-expressing cells (Dulin et al., 2018). Either dorsal or ventral donor grafts were transplanted into bilateral C5 dorsal column lesions (n = 5 for each group); all animals underwent peripheral preconditioning lesions on the same day. Animals were sacrificed 6 weeks later. Analysis of grafts demonstrated that ventral grafts were nearly depleted of TLX3-expressing sensory interneurons (Figure 4A), whereas dorsal grafts were enriched in TLX3-expressing domains (Figures 4B and 4C). The mean area of the dorsal grafts occupied by TLX3-expressing cell clusters was 13.1% ± 0.5%, compared with 1.3% ± 0.2% in ventral grafts (n = 5 for each group). We also quantified the mean area of whole grafts occupied by TLX3-expressing cell clusters from the first rat experiment (above): 8.8% ± 0.5% of whole E14 spinal cord grafts contained TLX3-expressing regions in animals with conditioning lesions, and 8.5% ± 0.9% of whole E14 spinal cord grafts contained TLX3-expressing regions in animals without conditioning lesions. Thus, conditioning lesions do not amplify the area of graft that expresses TLX3, but E14 partitioning into ventral and dorsal halves significantly increases TLX3-expressing cell clusters in the dorsal-originating grafts.

Next we quantified sensory (CGRP) axon regeneration into dorsal versus ventral grafts (both groups had conditioning lesions). Overall, a mean area of 13.7% ± 1.2% of dorsal sensory grafts was occupied by CGRP axons, compared with 0.8% ± 0.2% of ventral grafts (n = 5 for each group, $p < 0.001$, Student's t test; Figures 4D–4K). Among earlier animals with whole grafts, a mean area of 8.1% ± 1.7% of grafts was occupied by CGRP axons in animals with conditioning lesions (Figure 2L), and a mean area of 0.9% ± 0.1% of grafts was occupied by CGRP axons in animals without conditioning lesions (Figure 2L). Indeed, the total graft area containing regenerating sensory axons increased 1.6-fold in animals with dorsal grafts with conditioning lesions (Figure 4K), compared with animals that received whole grafts with conditioning lesions (Figure 2L). Thus, the combination of altering the intrinsic

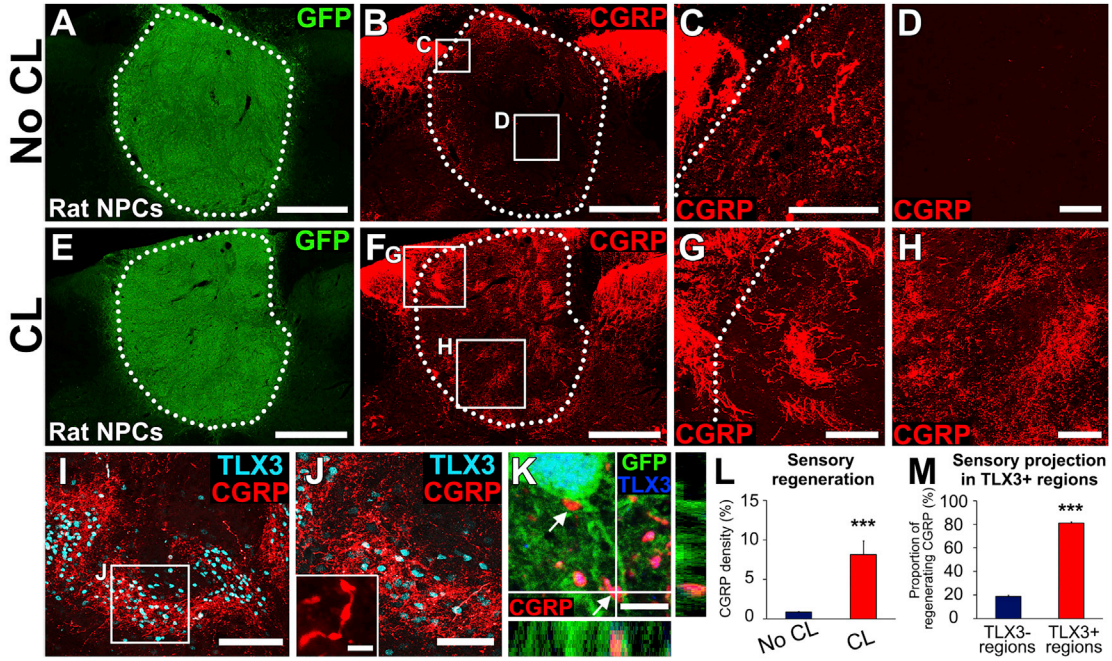

Figure 2. Conditioning Lesions Induce Robust Sensory Axon Regeneration into Rat Neural Progenitor Cell Grafts

(A–D) Graft of rat multipotent NPCs in C5 dorsal column lesion site of the rat spinal cord, 6 weeks post grafting. No conditioning lesion. (A) Graft (GFP) fills lesion site. Scale bar, 500 μm. (B) As in the primate, host sensory axons labeled for CGRP regenerate into the NPC grafts, but growth is limited to superficial regions of the graft; the amount of host sensory axon regeneration into the core of the graft is very modest. Dotted lines indicate host/graft interface. Scale bar, 500 μm. Boxed areas are shown in (C) and (D). (C) Host sensory axons only regenerate into superficial graft regions closely apposed to host. Scale bar, 100 μm. (D) Graft core is devoid of regenerating sensory axons. Scale bar, 100 μm.

(E–H) Graft of rat multipotent NPC graft in C5 dorsal column lesion site with a conditioning lesion. (E) Graft (GFP) fills lesion site. Scale bar, 500 μm. (F) After conditioning lesions, grafts are far more extensively penetrated by host sensory axons. Scale bar, 500 μm. Dotted line indicates host/graft interface. (G and H) Higher-magnification views show extensive regeneration of host sensory axons into graft, including regions well within graft core (H). Scale bars, 100 μm.

(I and J) As in the primate, host sensory axons regenerate nearly exclusively into TLX3-expressing cell clusters in grafts (cyan) (I). Scale bar, 100 μm. (J) Higher magnification of TLX3-expressing cell region from (I). Scale bar, 50 μm. Inset shows bouton-like swellings on CGRP-expressing axons; scale bar, 2 μm.

(K) Regenerating host axons form close appositions with soma and dendrites (arrows) of TLX3-expressing neurons in graft (blue). Scale bar, 2 μm.

(L) Host sensory axon regeneration increases nearly 9.6-fold following placement of conditioning lesions (n = 5 for each group). Data are presented as mean ± SEM. ***p < 0.001, Student's t test.

(M) Most regenerating host sensory axons penetrate regions of TLX3-expressing cell clusters in grafts (n = 5 for each group). Data are presented as mean ± SEM. ***p < 0.001, Student's t test.

growth state of the neuron by applying conditioning lesions, plus enriching the graft environment with appropriate sensory neuronal targets, resulted in maximal and extensive sensory axonal regeneration into grafts. Moreover, depleting a graft of sensory neuronal targets also markedly attenuated host axon regeneration into grafts.

DISCUSSION

The manipulation of intrinsic growth state is a powerful strategy to enhance axonal regeneration in the injured adult CNS (He and Jin, 2016). We now show that activating the intrinsic growth state of the injured neuron can also robustly amplify host regeneration into a NPC graft: both the total density and distance of host axons regenerating into the graft are enhanced. These regenerating host axons (labeled for CGRP) project to phenotypically appropriate interneuronal targets (expressing TLX3) in the graft (Dulin et al., 2018), and maintain this appropriate pattern of projection after enhancement of the intrinsic growth state. Taking advantage of appropriate target finding by host axons regenerating into grafts, we can further increase the density of host axon regeneration by enriching grafts

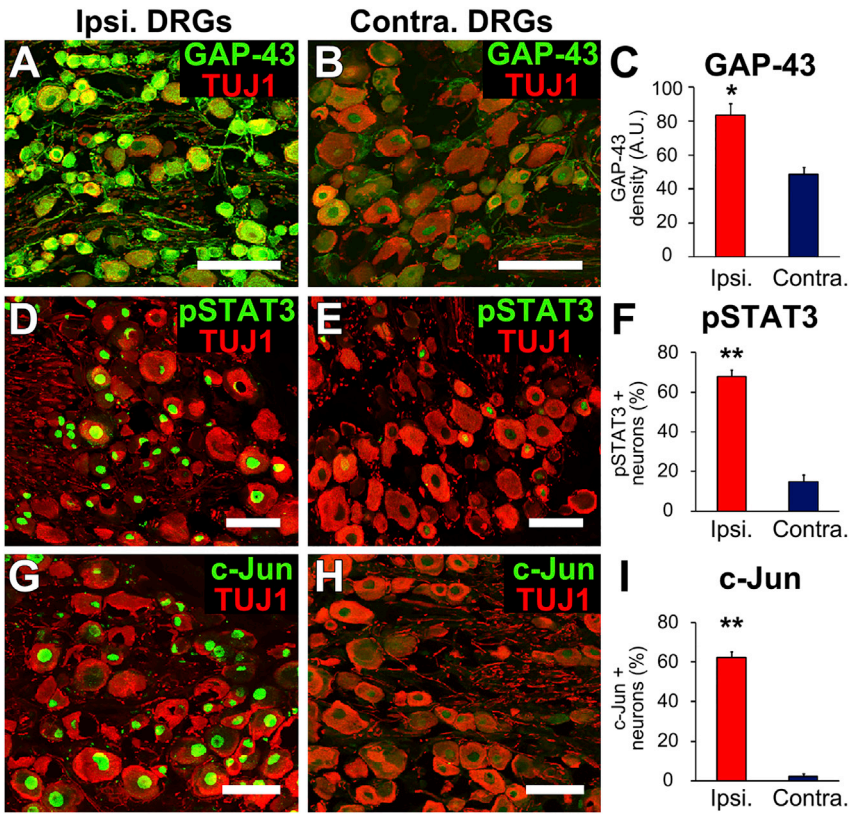

Figure 3. Conditioning Lesions Activate Intrinsic Neuronal Growth State

(A–C) Seven days after a peripheral conditioning lesion, GAP-43 expression (green) is significantly upregulated in ipsilateral DRGs at C7 (A) compared with contralateral DRGs (B), quantified in (C) (n = 3 replicates). TUJ1 is a mature neuronal marker.

(D–I) Conditioning lesions also upregulate expression of (D–F) pSTAT3 and (G–I) c-Jun in conditioned DRGs (n = 3).

Data are presented as mean ± SEM. *p < 0.05, **p < 0.01, Student's t test. Scale bars, 100 μm.

with appropriate target domains. Collectively, these findings demonstrate that host axon regeneration into NPC grafts can be both amplified and shaped by changing the intrinsic growth state of the host neuron, and by modifying the neuronal constituents of grafts. Moreover, we show that host axon regeneration into grafts can be attenuated by depleting grafts of appropriate target neurons. In theory, future attempts to maximize the functional efficacy of grafts could be achieved by enriching grafts with appropriate target neurons for some neural systems, such as motor interneurons, while attenuating the number of neurons in grafts that could result in dysfunctional outcomes, such as interneuronal targets of nociceptive systems. Future experiments will test these hypotheses as we work toward identifying the optimal set of neuronal constituents in grafts that will improve motor and useful sensory outcomes (e.g., proprioceptive and touch modalities, but not pain systems).

Activation of the intrinsic growth state of the neuron was achieved in this study using conditioning lesions, a classic technique that has proved mechanistically informative in many previous studies (Blesch et al., 2012; Kadoya et al., 2009; Ma et al., 2000; Neumann and Woolf, 1999; Qiu et al., 2002; Woolf, 2001). However, the use of a peripheral conditioning lesion also precluded the study of functional outcomes in this experiment, because the peripheral nerves were injured. Other approaches to activating the intrinsic growth state of the neuron that are more clinically practical can be utilized in future studies, e.g., the orally available drug ambroxol (Chandran et al., 2016) or other pharmacological agents currently under study.

How are axons guided to appropriate target neurons in the neural stem cell graft? During neural development, axon guidance occurs either as a result of attraction or repulsion mediated by diffusible guidance molecules, by guideposts in the extracellular matrix, or by binding of receptor-ligand pairs between cells and axons (Giger et al., 2010; Hilton and Bradke, 2017). Several guidance cues persist in the adult CNS, including semaphorin 3a and Wnts, among other molecules (Liu et al., 2008; Meyer, 2014). We hypothesize that the persistence or re-expression of these guidance mechanisms after injury in the adult CNS, combined with active guidance mechanisms present in the graft, mediate successful axon guidance in neural stem cell grafts. Future work will attempt to identify precise cellular mechanisms mediating these effects.

EXPERIMENTAL PROCEDURES

A detailed description of experimental procedures is given in Supplemental Information.

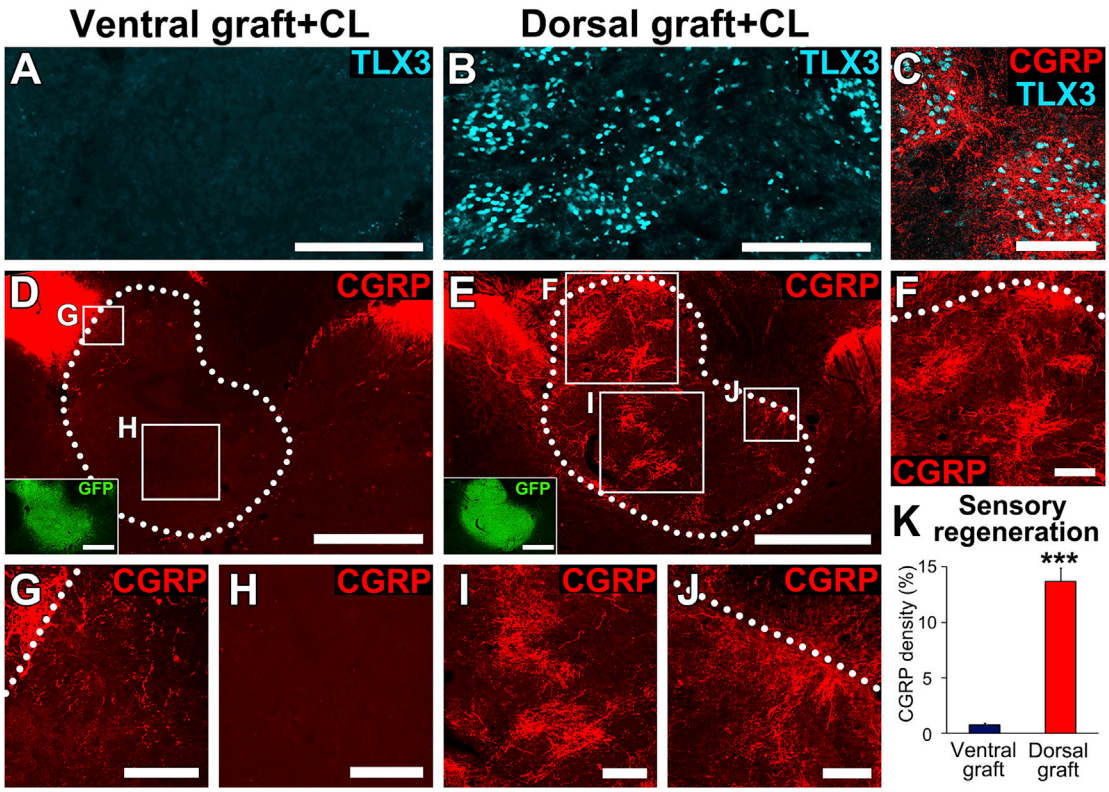

Figure 4. Graft Enrichment with Appropriate Target Domains Enhances Host Regeneration

(A and B) Grafts of (A) ventral E14 multipotent NPCs are markedly depleted of TLX3-expressing neurons, the targets of regenerating sensory axons, while dorsal grafts (B) are enriched in TLX3-expressing neurons. Scale bars, 200 μm.

(C) Regenerating sensory axons labeled for CGRP preferentially innervate TLX3-expressing domains in dorsal grafts. Scale bar, 100 μm.

(D–J) Transverse sections at C5 labeled for CGRP. (D) Grafts of ventral E14 multipotent NPCs, which are depleted in target neurons of primary sensory afferents, show nearly no penetration by regenerating host sensory axons, even when a conditioning lesion has been applied. Scale bar, 500 μm. Inset shows GFP labeling of the same section; scale bar, 500 μm. Higher magnification is shown in (G) and (H). Scale bars, 50 μm (G) and 200 μm (H). (E) In contrast, dorsal E14 multipotent NPC grafts, which are enriched in target neurons of primary sensory afferents, are extensively penetrated by regenerating host sensory axons at all depths. A conditioning lesion was applied. Scale bar, 500 μm. Inset shows GFP labeling of the same section; scale bar, 500 μm. Higher magnification is shown in (F), (I), and (J). Scale bars, 100 μm.

(K) Quantification demonstrates that sensory axonal regeneration is markedly depleted in ventral grafts, and increased in dorsal grafts ($n = 5$ for each group; $^{***}p < 0.001$, Student's t test), even when compared with whole E14 multipotent NPCs. Data are presented as mean ± SEM.

Animals

We studied five male rhesus macaques (*Macaca mulatta*, 7–9 years old, 8.5–11 kg) and 23 adult female Fischer 344 rats (150–250 g; The Jackson Laboratory, Bar Harbor, ME). All surgeries were approved by the Institutional Animal Care and Use Committee of the respective institutions housing the animals. NIH guidelines for laboratory animal care and safety were strictly followed.

Primate Surgery and Human NPC Preparation

The monkeys described here were reported previously (Rosenzweig et al., 2018) and surgical procedures for placement of right C7 hemisection lesions were described previously (Rosenzweig et al., 2018). GFP-expressing human fetal spinal cord neural stems (NSI-566RSC-GFP) were a gift of NeuralStem, and culture methods were reported previously (Lu et al., 2012). Three to nine months after grafting, subjects were very deeply anesthetized and then transcardially perfused with 4% paraformaldehyde (PFA), and the spinal cords were removed and sectioned into 30-μm-thick horizontal sections.

Rodent Surgery and Rat NPC Preparation

C5 bilateral dorsal column wire knife lesions were made as described previously (Kadoya et al., 2016) and left peripheral nerve transections were performed as described previously (Wang et al., 2008). Rat multipotent NPCs were prepared from E14 F344 developing rat spinal cords as described previously (Dulin et al., 2018; Lu et al., 2012). In all cases, 1.0×10^6 viable cells were grafted into the lesion cavity. Animals were transcardially perfused with 4% PFA,

post-fixed in 4% PFA overnight, and immersed in 30% sucrose for 2 days. Spinal cord tissues were cut into 30-μm-thick transverse free-floating sections and DRGs were sectioned at 10-um-thick intervals and directly mounted onto gelatin-coated slides.

Immunohistochemistry

Sections or slides were incubated with primary antibodies overnight and then incubated with secondary antibodies for 1 hr. For DRG labeling, heat-induced antigen retrieval was performed in the sodium citrate buffer at 90°C for 30 min. For CGRP labeling of spinal cord sections, the CGRP signal was amplified by the tyramide signal amplification method.

Statistical Analysis

Statistical analysis was performed using Student's t test. $p < 0.05$ was considered statistically significant. Data are presented as mean ± SEM.

SUPPLEMENTAL INFORMATION

Supplemental Information includes Supplemental Experimental Procedures and one figure and can be found with this article online at https://doi.org/10.1016/j.stemcr.2018.08.009.

AUTHOR CONTRIBUTIONS

H.K. designed and carried out most experiments, interpreted results, and wrote the manuscript. P.L. contributed to the rat cell graft experiment and the conception of the project, and wrote the manuscript. E.S.R. contributed to the human cell graft experiment and edited the manuscript. M.H.T. contributed to the conception of the project, the human cell graft experiment, and interpretation of results, and wrote the manuscript.

ACKNOWLEDGMENTS

We thank L. Graham, E. Staufenberg, and J. Weber for technical assistance; T. Müller and C. Birchmeier, Max-Delbrück-Center for Molecular Medicine, Berlin, Germany, for providing TLX3 antibody. Human 566RSC-UBQT NPCs were a gift from NeuralStem. Supported by the Veterans Administration Gordon Mansfield Spinal Cord Injury Consortium IP50RX001045 (to M.H.T.); the NIH (NS042291, NS104442, and EB014986, to M.H.T.); the Craig H. Neilsen Foundation (to H.K. and P.L.); the Japan Society for the Promotion of Science (to H.K.); the Bernard and Anne Spitzer Charitable Trust (to M.H.T.); the Dr. Miriam and Sheldon G. Adelson Medical Research Foundation (to M.H.T.); and the California National Primate Research Center funded by the NIH (NCRR P51 OD011107-56).

Received: March 28, 2018
Revised: August 8, 2018
Accepted: August 9, 2018
Published: September 6, 2018

REFERENCES

Adler, A.F., Lee-Kubli, C., Kumamaru, H., Kadoya, K., and Tuszynski, M.H. (2017). Comprehensive monosynaptic rabies virus mapping of host connectivity with neural progenitor grafts after spinal cord injury. Stem Cell Reports *8*, 1525–1533.

Alto, L.T., Havton, L.A., Conner, J.M., Hollis, E.R., Blesch, A., and Tuszynski, M.H. (2009). Chemotropic guidance facilitates axonal regeneration and synapse formation after spinal cord injury. Nat. Neurosci. *12*, 1106–U1108.

Blesch, A., Lu, P., Tsukada, S., Alto, L.T., Roet, K., Coppola, G., Geschwind, D., and Tuszynski, M.H. (2012). Conditioning lesions before or after spinal cord injury recruit broad genetic mechanisms that sustain axonal regeneration: superiority to camp-mediated effects. Exp. Neurol. *235*, 162–173.

Bunge, M.B. (2001). Bridging areas of injury in the spinal cord. Neuroscientist *7*, 325–339.

Chandran, V., Coppola, G., Nawabi, H., Omura, T., Versano, R., Huebner, E.A., Zhang, A., Costigan, M., Yekkirala, A., Barrett, L., et al. (2016). A systems-level analysis of the peripheral nerve intrinsic axonal growth program. Neuron *89*, 956–970.

Chong, M.S., Fitzgerald, M., Winter, J., Hu-Tsai, M., Emson, P.C., Wiese, U., and Woolf, C.J. (1992). GAP-43 mRNA in rat spinal cord and dorsal root ganglia neurons: developmental changes and re-expression following peripheral nerve injury. Eur. J. Neurosci. *4*, 883–895.

Dulin, J.N., Adler, A.F., Kumamaru, H., Poplawski, G.H.D., Lee-Kubli, C., Strobl, H., Gibbs, D., Kadoya, K., Fawcett, J.W., Lu, P., et al. (2018). Injured adult motor and sensory axons regenerate into appropriate organotypic domains of neural progenitor grafts. Nat. Commun. *9*, 84.

Fawcett, J.W. (2006). Overcoming inhibition in the damaged spinal cord. J. Neurotrauma *23*, 371–383.

Filbin, M.T. (2003). Myelin-associated inhibitors of axonal regeneration in the adult mammalian CNS. Nat. Rev. Neurosci. *4*, 703–713.

Giger, R.J., Hollis, E.R., 2nd, and Tuszynski, M.H. (2010). Guidance molecules in axon regeneration. Cold Spring Harb. Perspect. Biol. *2*, a001867.

He, Z.G., and Jin, Y.S. (2016). Intrinsic control of axon regeneration. Neuron *90*, 437–451.

Hilton, B.J., and Bradke, F. (2017). Can injured adult CNS axons regenerate by recapitulating development? Development *144*, 3417–3429.

Hur, E.M., Saijilafu, and Zhou, F.Q. (2012). Growing the growth cone: remodeling the cytoskeleton to promote axon regeneration. Trends Neurosci. *35*, 164–174.

Kadoya, K., Lu, P., Nguyen, K., Lee-Kubli, C., Kumamaru, H., Yao, L., Knackert, J., Poplawski, G., Dulin, J.N., Strob, H., et al. (2016). Spinal cord reconstitution with homologous neural grafts enables robust corticospinal regeneration. Nat. Med. *22*, 479–487.

Kadoya, K., Tsukada, S., Lu, P., Coppola, G., Geschwind, D., Filbin, M.T., Blesch, A., and Tuszynski, M.H. (2009). Combined intrinsic and extrinsic neuronal mechanisms facilitate bridging axonal regeneration one year after spinal cord injury. Neuron *64*, 165–172.

Laabs, T., Carulli, D., Geller, H.M., and Fawcett, J.W. (2005). Chondroitin sulfate proteoglycans in neural development and regeneration. Curr. Opin. Neurobiol. *15*, 116–120.

Lee, J.K., Geoffroy, C.G., Chan, A.F., Tolentino, K.E., Crawford, M.J., Leal, M.A., Kang, B., and Zheng, B.H. (2010). Assessing spinal axon regeneration and sprouting in Nogo-, MAG-, and OMgp-deficient mice. Neuron *66*, 663–670.

Liu, Y.B., Wang, X.F., Lu, C.C., Kerman, R., Steward, O., Xu, X.M., and Zou, Y.M. (2008). Repulsive Wnt signaling inhibits axon regeneration after CNS injury. J. Neurosci. *28*, 8376–8382.

Lu, P., Ceto, S., Wang, Y.Z., Graham, L., Wu, D., Kumamaru, H., Staufenberg, E., and Tuszynski, M.H. (2017). Prolonged human neural stem cell maturation supports recovery in injured rodent CNS. J. Clin. Invest. *127*, 3293–3305.

Lu, P., Wang, Y., Graham, L., McHale, K., Gao, M., Wu, D., Brock, J., Blesch, A., Rosenzweig, E.S., Havton, L.A., et al. (2012). Long-distance growth and connectivity of neural stem cells after severe spinal cord injury. Cell *150*, 1264–1273.

Lu, P., Woodruff, G., Wang, Y., Graham, L., Hunt, M., Wu, D., Boehle, E., Ahmad, R., Poplawski, G., Brock, J., et al. (2014). Long-distance axonal growth from human induced pluripotent stem cells after spinal cord injury. Neuron *83*, 789–796.

Ma, D., Connors, T., Nothias, F., and Fischer, I. (2000). Regulation of the expression and phosphorylation of microtubule-associated protein 1B during regeneration of adult dorsal root ganglion neurons. Neuroscience *99*, 157–170.

Mar, F.M., Bonni, A., and Sousa, M.M. (2014). Cell intrinsic control of axon regeneration. EMBO Rep. *15*, 254–263.

Meyer, M.A. (2014). Identification of 17 highly expressed genes within mouse lumbar spinal cord anterior horn region from an in-situ hybridization atlas of 3430 genes: implications for motor neuron disease. Neurol. Int. *6*, 5367.

Neumann, S., and Woolf, C.J. (1999). Regeneration of dorsal column fibers into and beyond the lesion site following adult spinal cord injury. Neuron *23*, 83–91.

O'Shea, T.M., Burda, J.E., and Sofroniew, M.V. (2017). Cell biology of spinal cord injury and repair. J. Clin. Invest. *127*, 3265–3276.

Qiu, J., Cai, C.M., Dai, H.N., McAtee, M., Hoffman, P.N., Bregman, B.S., and Filbin, M.T. (2002). Spinal axon regeneration induced by elevation of cyclic AMP. Neuron *34*, 895–903.

Rosenzweig, E.S., Brock, J.H., Lu, P., Kumamaru, H., Salegio, E.A., Kadoya, K., Weber, J.L., Liang, J.J., Moseanko, R., Hawbecker, S., et al. (2018). Restorative effects of human neural stem cell grafts on the primate spinal cord. Nat. Med. *24*, 484–490.

Seijffers, R., Mills, C.D., and Woolf, C.J. (2007). ATF3 increases the intrinsic growth state of DRG neurons to enhance peripheral nerve regeneration. J. Neurosci. *27*, 7911–7920.

Silver, J., Schwab, M.E., and Popovich, P.G. (2014). Central nervous system regenerative failure: role of oligodendrocytes, astrocytes, and microglia. Cold Spring Harb. Perspect. Biol. *7*, a020602.

Tedeschi, A., and Bradke, F. (2017). Spatial and temporal arrangement of neuronal intrinsic and extrinsic mechanisms controlling axon regeneration. Curr. Opin. Neurobiol. *42*, 118–127.

Wang, H., Spinner, R.J., Sorenson, E.J., and Windebank, A.J. (2008). Measurement of forelimb function by digital video motion analysis in rat nerve transection models. J. Peripher. Nerv. Syst. *13*, 92–102.

Woolf, C.J. (2001). Turbocharging neurons for growth: accelerating regeneration in the adult CNS. Nat. Neurosci. *4*, 7–9.

Stem Cell Reports, Volume *11*

Supplemental Information

Activation of Intrinsic Growth State Enhances Host Axonal Regeneration into Neural Progenitor Cell Grafts

Hiromi Kumamaru, Paul Lu, Ephron S. Rosenzweig, and Mark H. Tuszynski

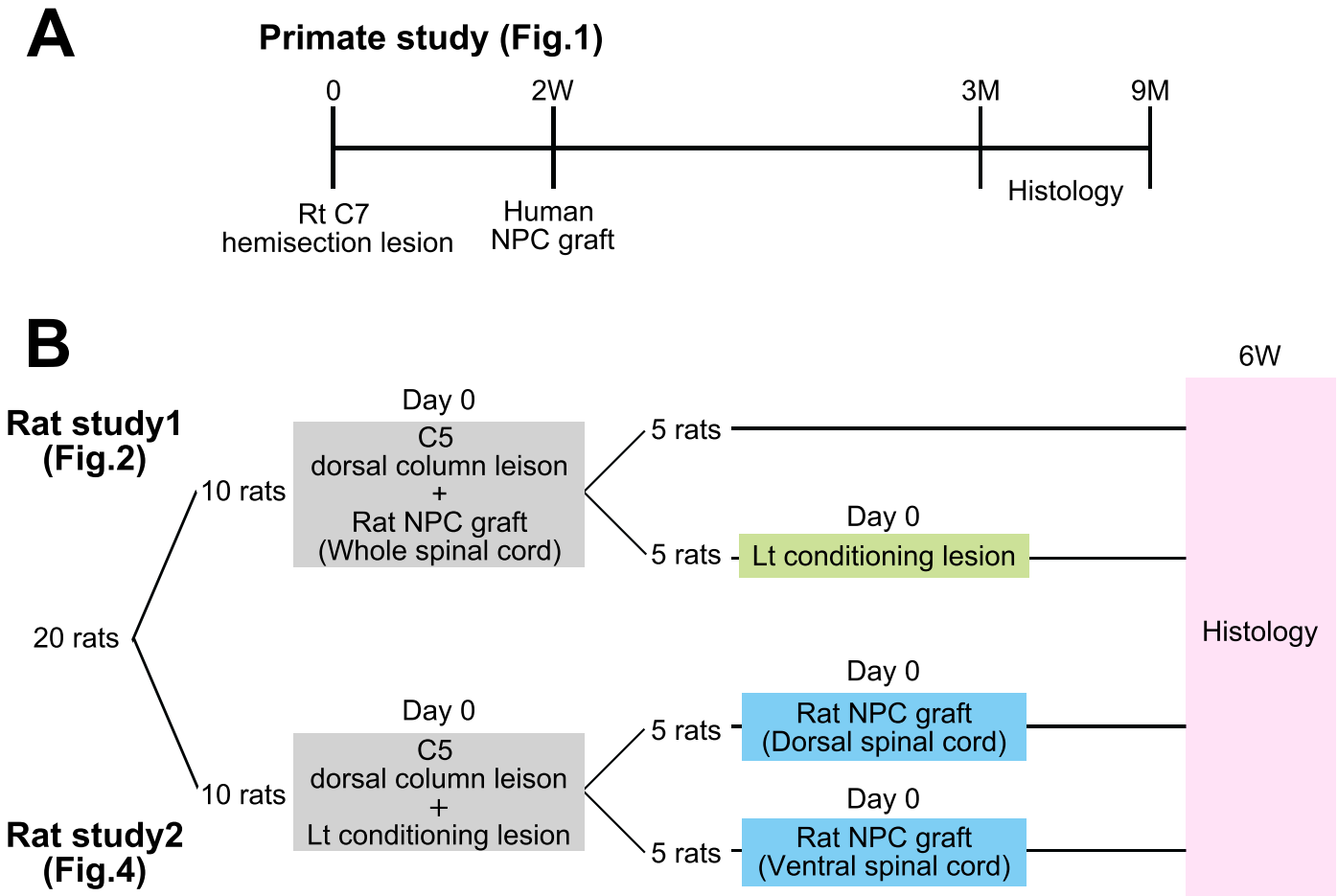

Figure S1. Study Schematic
(**A**) Primate study
(**B**) Rat study

Supplemental Experimental Procedures

Animals

Primate Studies: We studied five male rhesus macaques (*Macaca mulatta*, 7-9 -year-old, 8.5-11 kg). Subjects were housed at the California National Primate Research Center (Davis, CA). All surgery was done under deep anesthesia with 1.5–2.5% isoflurane. Tissue processing and analysis was performed at the Center for Neural Repair (University of California, San Diego; La Jolla, CA).

Rat Studies: A total of 23 adult female Fischer 344 rats (150-250g, The Jackson Laboratory, Bar Harbor, ME) were used in this study. Animals had free access to food and water throughout the study. All surgery was done under anesthesia using a combination (2 ml/kg) of ketamine (25 mg/ml), xylazine (1.3 g/ml), and acepromazine (0.25 mg/ml). All surgeries were approved by the Institutional Animal Care and Use Committee of the Department of Veterans Affairs (VA) San Diego Healthcare System. National Institutes of Health guidelines for laboratory animal care and safety were strictly followed.

Primate Study

The monkeys described here were reported previously (Rosenzweig et al., 2018). GFP-expressing human fetal spinal cord neural stems (NSI-566RSC-GFP) were a gift of NeuralStem, Inc. Culture methods were reported previously (Lu et al., 2012). Briefly, the cervical and upper thoracic human fetal spinal cord from a single week 8 gastrulation male donor was dissociated and suspended in serum-free DMEM/F12 media containing N2 supplement, 100 mg/l human plasma apo-transferrin, 25 mg/l recombinant human insulin, 1.56 g/l glucose, 20 nM progesterone, 100 mM putrescine, and 30 nM sodium selenite. Cells were plated on 100 mg/ml poly-D-lysine coated flasks and expanded. 10 ng/ml FGF2 was added every other day. Cells were replated when they reached 75% confluence. At each passage, cells were harvested and stored in liquid nitrogen. For shipping, cells were thawed 1 day prior to grafting, washed, and shipped overnight at 2-8°C. Surgical procedures for placement of right C7 hemisection lesions were described previously (Rosenzweig et al., 2018). Briefly, after deep anesthesia, a C5 laminectomy was performed and a right lateral hemisection was created in the underlying C7 spinal cord. Two weeks after the C7 hemisection, twenty million human fetal spinal cord neural progenitor cells were suspended in a fibrin matrix containing a cocktail of growth factors, including brain-derived neurotrophic factor (BDNF; 50 μg/mL, Peprotech, Rocky Hill, NJ), neurotrophin-3 (NT-3; 50 μg/mL, Peprotech), glial cell-derived neurotrophic factor (GDNF; 10 μg/mL, Sigma**,** St. Louis, MO), epidermal growth factor (EGF; 10 μg/mL, Sigma), basic fibroblast growth factor (bFGF; 10 μg/mL, Sigma), acidic FGF (aFGF; Sigma, 10 μg/mL), hepatocyte growth factor (HGF; 10 μg/mL, Sigma), insulin-like growth factor 1 (IGF-1; 10 μg/mL, Sigma), platelet-derived growth factor (PDGF-AA; 10 μg/mL, Peprotech), vascular endothelial growth

factor (VEGF; 10 μg/mL, Peprotech), and a calpain inhibitor (MDL28170, 50 μM, Sigma) (Lu et al., 2012). The cell / growth factor mix were injected into the lesion site. After grafting, animals received a 3-drug immunosuppressive regimen consisting of mycophenolate modafeniul (MMF; CellSept, the initial dose, 50 mg/kg twice a day), tacrolimus (FK-506; ProGraf, the initial dose, 0.5 mg/kg twice a day), and prednisone (The initial dose, 2 mg/kg/day; the maintenance dose1 mg/kg/day). Dosages of MMF and FK-506 were adjusted based on their blood concentration. After three to nine months, subjects were transcardially perfused with 4% paraformaldehyde (PFA), and the spinal cords were removed and sectioned into 30-μm-thick horizontal sections. Two sections per animal were labeled for calcitonin gene-related peptide (CGRP) regeneration using Green fluorescence protein (GFP, chicken, Aves Labs GFP-1020, 1:2000), CGRP (mouse, GeneTex GTX82726, 1:500), and NeuN (mouse, Millipore MAB377, 1:500) antibodies. For quantification of primate CGRP axonal regeneration into the human graft, whole graft images were sampled using the BZ-9000 digital microscope system (N = 5, 2 sections per monkey). GFP + area was outlined and inner contour lines were drawn at 100 μm intervals from the surface of the graft. CGRP intensity was thresholded and total CGRP density in the total GFP + area and each area (0-100um, 101-200um, 201-300um, 301-400um, 401-500um, 501- um from the surface) was calculated using ImageJ. The phenotype of grafted neurons penetrated by regenerating host sensory axons was identified by immunolabeling for TLX3 (generous gift from T. Müller and C. Birchmeier, Max-Delbrück-Center for Molecular Medicine, Berlin, Germany), a transcription factor that is specifically expressed by spinal sensory neurons. For quantification of CGRP density in TLX3 + domains, images were sampled using the confocal microscope (200x magnification, N = 5, 2 fields, 2 sections per monkey). TLX3 + domains were outlined using ImageJ. CGRP intensity was thresholded and their density was calculated in each region of interest (TLX3+) and remaining region (TLX3-). Statistical analysis was performed using the Student's T-test. $P < 0.05$ was considered statistically significant. Data are presented as mean ± standard error of the mean (SEM).

Rodent Study

In **Study 1** (**Fig. 2**), we examined the effects of peripheral conditioning lesions on the regeneration of sensory axons into neural progenitor cell grafts placed into sites of SCI. A total of ten F344 rats underwent C5 bilateral dorsal spinal cord lesions; two weeks later, these animals received grafts of E14 spinal cord-derived multipotent neural progenitor cells into the lesion site. Half of these animals (N = 5) also received peripheral nerve conditioning lesions at the time of grafting; conditioning lesions were created by transecting the left musculocutaneous, median, ulnar, and radial nerves, ensuring that all axons projecting into the C5 spinal cord segment were conditioned (Wang et al., 2008). In **Study 2** (**Fig. 4**), we studied the effects of enriching grafts with more targets for regenerating host sensory axons. Ten F344 rats underwent C5 bilateral dorsal column spinal cord lesions, with neural progenitor cell grafts and

conditioning lesions, as described above. In this study, the neural progenitor cell grafts were either enriched or depleted of appropriate targets for regenerating sensory neurons by grafting either the *dorsal* half of the developing E14 spinal cord (enriched in sensory neuronal targets, N = 5 animals), or the *ventral* half of the developing E14 spinal cord (depleted in sensory neuronal targets, N = 5 animals). In all studies, animals were sacrificed six weeks after grafting.

Peripheral nerve surgery, Spinal cord lesions, and Rat NPC preparation

Peripheral nerve transection was performed as described previously, with a slight modification (Wang et al., 2008). The musculocutaneous, median, and ulnar nerves in the left forelimb were exposed through a medial longitudinal incision above the elbow. The ulnar and median nerves were transected at the level of the medial epicondyle and the musculocutaneous nerve was transected above the elbow. After transection of these three nerves, the radial nerve was exposed and transected after developing the interval between the biceps muscles and the humeral shaft. We placed the conditioning lesions on the same day as the spinal cord injury (Blesch et al., 2012). Conditioning lesions were placed on only on one side (left) because subjects require one functional forelimb to eat and groom. The functional forelimb without a conditioning lesion served as a control for analysis of growth-associate gene expression analysis after conditioning lesions in affected forelimb. Due to the peripheral nerve transections, we could not examine functional outcomes in this study.

Lesions: Rat C5 bilateral dorsal column wire knife lesions were made as described previously (Kadoya et al., 2016). Briefly, the spinal cord dorsal surface was exposed by C5 laminectomy. The tungsten wire knife was inserted 1 mm from the dorsal surface and raised; the most dorsal aspect of the dorsal column was left uncut to support graft retention without the need for growth factor supplementation (Kadoya et al., 2016).

Grafts: Multipotent neural progenitor cell grafts were prepared from E14 F344 developing rat spinal cords as described previously (Lu et al., 2012). Briefly, E14 spinal cords were carefully dissected out to avoid any dorsal root ganglia (DRG) tissue contamination. Dissected spinal cords were treated with 0.125% trypsin were mechanically dissociated into single cells and then filtered with a 40 um cell strainer. These multipotent neural progenitor cell grafts were re-suspended to a concentration of 5.0×10^5 cells/µl in phosphate buffered saline. For dorsal and ventral spinal grafts, the spinal cords were opened in the middle of dorsal plane and then separated into dorsal and ventral halves. Cell viability was measured with trypan blue exclusion (Thermo fisher scientific, Waltham, MA): in all cases, graft viability exceeded 90%. In all experiments, 1.0×10^6 viable cells were grafted into the lesion cavity, through the dura, using a pulled glass micropipette and a PicoSpritzer II (General Valve, Inc., Fairfield, NJ). After six-week survival period, animals were transcardially perfused with 4% PFA and post-fixed in 4% PFA overnight.

Immunohistochemistry: Fixed tissues were immersed in 30% sucrose for two days. Spinal cord tissues were cut into 30-μm-thick transverse free-floating sections. DRGs were sectioned at 10-um-thick intervals and directly mounted onto gelatin-coated slides. Sections were incubated with primary antibodies against GFP, CGRP, NeuN, TLX3, c-Jun (mouse, Santa Cruz Biotechnology sc-74543, 1:200), phospho- signal transducer and activator of transcription 3 (pSTAT3: rabbit, Cell Signaling 9145S, 1:200), growth associated protein 43 (GAP-43, rabbit, Abcam ab75810, 1;200), or beta-III Tubulin (TUJ1, mouse, BioLegend 801202, 1:200) overnight and then incubated with Alexa 488, 568, or 647 conjugated donkey secondary antibodies (1:500, Invitrogen, Carlsbad, CA) and DAPI (1:1000, Invitrogen) for 1 hr. For DRG labeling, heat-induced antigen retrieval was performed in the sodium citrate buffer (10 mM sodium citrate (Sigma), 0.05% Tween 20 (Thermo fisher scientific), pH 6.0 at 90**°C** for 30 min. For CGRP labeling of spinal cord sections, the CGRP signal was amplified by the tyramide signal amplification method. Briefly, after incubation of primary antibody, sections were incubated with biotinylated donkey secondary antibodies (Jackson Immunoresearch, West Grove, PA) for 1 hr, ABC solution (Vector Laboratories, Burlingame, CA) for 30 min, biotinyl tyramide in tris-buffered saline (TBS) solution containing 0.1% H_2O_2 for 30 min, and then Alexa Fluor-conjugated streptavidin (Invitrogen) for 1 hr. Sections were washed with TBS three times between each step. Sections were mounted on glass slides and cover slipped with Mowiol mounting medium (Sigma). Images were captured using an Olympus AX-70 fluorescence microscope (Olympus, Tokyo, Japan*)* equipped with an Optronics Microfire A/R digital camera Microfire A/R, (Optronics, Goleta, CA), a confocal microscope (FV-1000, Olympus, Tokyo, Japan), or the BZ-9000 digital microscope system (Keyence, Osaka, Japan).

Quantification and Statistical Analysis

For quantification of sensory regeneration into the graft, whole graft images were sampled using the BZ-9000 digital microscope system (N = 5, 2-3 sections per rat). GFP + area was outlined, CGRP intensity was thresholded, and CGRP + area in the GFP + area (%) was calculated using ImageJ. For quantification of sensory density in TLX3 + regions, images were sampled using the confocal microscope (200x magnification, N = 5, 3 sections per animal). TLX3 + regions were outlined using ImageJ. CGRP intensity was thresholded and calculated in each region of interest (TLX3+) and remaining region (TLX3-).

For quantification of c-Jun, pSTAT3, GAP-43, and TUJ1 in DRGs, whole DRG images were sampled using the Olympus AX-70 fluorescence microscope (100x magnification, N = 3, 4 sections per animal). c-Jun, pSTAT3, GAP-43, and TUJ1 signal intensity was thresholded using ImageJ. Total c-Jun, pSTAT3, and TUJ1 expressing cells were counted (**Fig.3B and C**) and GAP-43 intensity was normalized by TUJ1+ area (**Fig. 3A**).

Statistical analysis was performed using the Student's T-test. $P < 0.05$ was considered statistically

significant. Data are presented as mean ± standard error of the mean (SEM).